Reciprocal integrin/integrin antagonism through kindlin-2 and Rho GTPases regulates cell cohesion and collective migration

Ivo van der Bijl[a,1], Kalim Nawaz[a,1], Ugne Kazlauskaite[a], Anne-Marieke van Stalborch[a], Simon Tol[a], Ana Jimenez Orgaz[b], Iman van den Bout[b,c], Nathalie R. Reinhard[d], Arnoud Sonnenberg[b,2], Coert Margadant[a,b,e,2,*]

[a]Molecular Cell Biology, Sanquin Research, Plesmanlaan 125, 1066 CX, Amsterdam, The Netherlands
[b]Division of Cell Biology, The Netherlands Cancer Institute, Plesmanlaan 121, 1066 Amsterdam, CX, The Netherlands
[c]Department of Physiology, Faculty of Health Sciences, University of Pretoria, Private Bag X323 Pretoria, South Africa
[d]Department of Medical Biochemistry, Amsterdam University Medical Center, Meibergdreef 9, 1105 Amsterdam, AZ, the Netherlands
[e]Department of Molecular Cell Biology and Immunology, Amsterdam University Medical Center, De Boelelaan 1108, 1081 Amsterdam, HZ, the Netherlands

*Corresponding author at: Molecular Cell Biology and Immunology, Amsterdam University Medical Center, De Boelelaan 1108, 1081 HZ, Amsterdam, The Netherlands.email: c.margadant@sanquin.nl

[1]These authors contributed equally to this work.
[2]Co-senior authors.

Abstract

Collective cell behaviour during embryogenesis and tissue repair requires the coordination of intercellular junctions, cytoskeleton-dependent shape changes controlled by Rho GTPases, and integrin-dependent cell-matrix adhesion. Many different integrins are simultaneously expressed during wound healing, embryonic development, and sprouting angiogenesis, suggesting that there is extensive integrin/integrin cross-talk to regulate cell behaviour. Here, we show that fibronectin-binding β1 and β3 integrins do not act synergistically, but rather antagonize each other during collective cell processes in neuro-epithelial cells, placental trophoblasts, and endothelial cells. Reciprocal β1/β3 antagonism controls RhoA activity in a kindlin-2-dependent manner, balancing cell spreading, contractility, and intercellular adhesion. In this way, reciprocal β1/β3 antagonism controls cell cohesion and cellular plasticity to switch between extreme and opposing states, including epithelial versus mesenchymal-like phenotypes and collective versus individual cell migration. We propose that integrin/integrin antagonism is a universal mechanism to effectuate social cellular interactions, important for tissue morphogenesis, endothelial barrier function, trophoblast invasion, and sprouting angiogenesis.

Keywords: Collective cell migration; Epithelial-to-mesenchymal transition; Fibronectin; Inhibition of integrin function; Kindlin-2; Rho GTPases

Introduction

Collective cell behaviour is essential for the morphogenesis and maintenance of tissues, as well as for their remodeling during embryonic development, wound healing, trophoblast invasion, sprouting angiogenesis, and tumor metastasis. Many of these processes are characterized by high cellular plasticity in terms of gene expression and morphology, and involve dynamic interconversion between cellular phenotypes such as epithelial-to-

mesenchymal transition (EMT), or between collective and individual modes of cell migration [1,2]. Morphological changes at the single-cell level are mostly governed by re-organization of the actin cytoskeleton, under the control of Rho-family GTPases. While Rac promotes actin branching through the Arp-2/3 complex, leading to cell spreading and formation of lamellipodia, the Rho/Rho kinase (ROCK) pathway induces actomyosin-based cytoskeletal tension, resulting in the formation of actin stress fibers, cell contraction, and the generation of cellular forces necessary for migration [3], [4], [5], [6]. Individual cell-shape changes through Rho GTPases are tightly linked to intercellular adhesion mediated by transmembrane receptors of the cadherin family, and thus regulate collective cell behaviour [7,8]. For instance, sprouting vascular cells, migrating epithelial cell sheets, invasive tumor explants and organoids, and developing glands all require a tight balance between RhoA/ROCK signaling and Rac activity that determines individual versus collective cell migration, leader-follower hierarchy, and polarity and directionality [9], [10], [11], [12], [13], [14]. Likewise, the dynamic regulation of endothelial and epithelial barrier function relies on tight spatiotemporal control of Rho GTPase-regulated actin cytoskeletal organization and cadherins [15,16]. Thus, social cellular interactions are dynamically controlled by Rho GTPases, the cytoskeleton, and cell-cell junctions.

In addition, many of these events also depend on integrins, a family of 24 αβ heterodimeric transmembrane receptors that bind to proteins in the extracellular matrix (ECM), while their cytoplasmic tails associate with the actin cytoskeleton [17]. Integrin-ligand interactions stimulate the formation of adhesion complexes such as focal adhesions (FAs) and fibrillar adhesions (FBs), and elicit cell signaling, cytoskeletal reorganization, cell spreading, and migration [17]. Most integrin β-subunits contain two NPxY/NxxY motifs and an intervening threonine/serine (T/S)-rich region in their cytoplasmic tails, which regulate integrin activation through the binding of talins and kindlins [18]. Furthermore, these regions recruit a variety of regulatory, signaling, adaptor, and scaffolding proteins, thus regulating downstream signaling [18]. Integrin-ECM interactions can promote the assembly of intercellular adhesion complexes, but also cause their disruption through RhoA-dependent cytoskeletal tension, thus inducing a loss of cell-cell adhesion [19], [20], [21].

All adherent cells constitutively express a variety of different integrins, and many others are *de novo* expressed in pathological conditions or during embryonic development and tissue repair. Embryonic and wound-associated extracellular matrices are enriched in proteins with an arginine-glycine-aspartic acid (RGD) motif, such as fibronectin (FN) and fibrin [22,23]. The RGD sequence is recognized by several integrins containing the β1-subunit, as well as by αv integrins like αvβ3, expressed on a variety of cell types including fibroblasts, vascular endothelial cells, smooth muscle cells, and placental trophoblasts [24,25]. In solitary cells such as fibroblasts, RGD-binding integrins synergistically promote cell adhesion, adhesion strengthening, and rigidity sensing [26], [27], [28]. However, they can also behave very differently with regard to their dynamic behaviour in FAs, sensing and transduction of mechanical signals from the environment, FA turnover and migratory behaviour, or their traffic through the endolysosomal system [29], [30], [31], [32], [33], [34], [35]. We have previously shown that the expression of β1 versus β3 integrins into murine neuro-epithelial GE11 cells (creating GEβ1 and GEβ3 cells, respectively) induces extreme and opposing cellular phenotypes on FN, driven by the differential activation of Rho GTPases. While GEβ1 cells exhibit high RhoA-driven cell contractility, causing EMT-like morphological changes, cell-cell dissociation, and fast but random cell motility, GEβ3 cells support Rac-dependent cell spreading and cohesion, as well as collective and directional cell migration [36], [37], [38], [39], [40]. Although these data illustrate the individual roles of β1 versus β3 integrins, it

is less clear how these integrins interact with each other to regulate Rho GTPase activities and cross-talk to cell-cell junctions, thus controlling the phenotype and social behaviour of cell collectives.

Here we show that β1 and β3 integrins antagonize, rather than stimulate, each other's function in the regulation of intercellular adhesion and collective cell migration. β1 integrins attenuate αvβ3-dependent cell spreading and cell cohesion, by supporting RhoA-stimulated cell-cell contact disruption. In turn, αvβ3 counteracts β1-induced RhoA activation to limit contractility, which requires the cytoplasmic β3 motif recognized by kindlin-2. This reciprocal suppression of integrin function occurs in neuro-epithelial cells, endothelial cells, and trophoblasts, and regulates cell migration on FN, intercellular adhesion and monolayer integrity, and sprouting angiogenesis in fibrin gels.

Thus, our work uncovers a mechanism of reciprocal antagonism between different RGD-binding integrins, and shows that a tight balance between the differential effects of β1 and β3 is required to maintain cellular phenotype and collective cell behaviour.

Results

Reciprocal integrin antagonism dictates cell cohesion, Rho GTPase activation, and cell migration on FN

To investigate potential crosstalk between β3 and β1 integrins, we first expressed the human β3 subunit into GEβ1 cells by retroviral transduction (creating GEβ1/β3 cells), and isolated double-positive cells by FACS (Fig. 1a). Intriguingly, the expression of β3 into GEβ1 cells increased cell spreading on FN, but not as much as in the absence of β1, indicating that β1 integrins limit αvβ3-induced cell spreading (Fig. 1b and c). In addition, GEβ1/β3 cells were not organized in islands, and exhibited a morphology with contractile protrusions (quantified by measuring the cell 'circularity'), reminiscent of GEβ1 (Fig. 1b and c). Upon seeding onto FN, all cell lines comparably supported Rac activation, but the high RhoA activation promoted by β1 integrins was attenuated by αvβ3 (Fig. 1d; Suppl. Fig. 1a). We next investigated migratory behaviour in scratch assays. As observed earlier, GEβ3 cells migrated collectively (i.e. maintaining cell-cell contacts during migration) and in a directional manner, leading to fast scratch closure. In contrast, GEβ1 cells quickly lost contact with other cells and migrated fast but randomly, including parallel to the wound edges or even back into the monolayer, thereby delaying scratch closure (Supplementary Movie 1; Fig. 1e and f). Interestingly, GEβ1/β3 cells showed an intermediate phenotype; some loss of cell cohesion followed by random cell migration was observed, but this was not as pronounced as in GEβ1 cells, indicating that αvβ3 counteracts, at least partially, β1-induced cell-cell dissociation. As a result, the speed of scratch closure as well as the migration directionality were in between those of GEβ1 and GEβ3 cells (Supplementary Movie 1; Fig. 1e and f). We also analyzed single-cell migration on FN (5 μg/ml). As observed before, GEβ1 cells migrated fast but with low directionality, while the reverse was true for GEβ3 (Fig. 1g and h). In line with the cell spreading, Rho activation, and scratch assays, the migration velocity and directionality of GEβ1/β3 cells were in between those of GEβ1 and GEβ3, further suggesting that integrin αvβ3 and β1 integrins antagonize each other's function (Supplementary Movie 2; Fig. 1g and h).

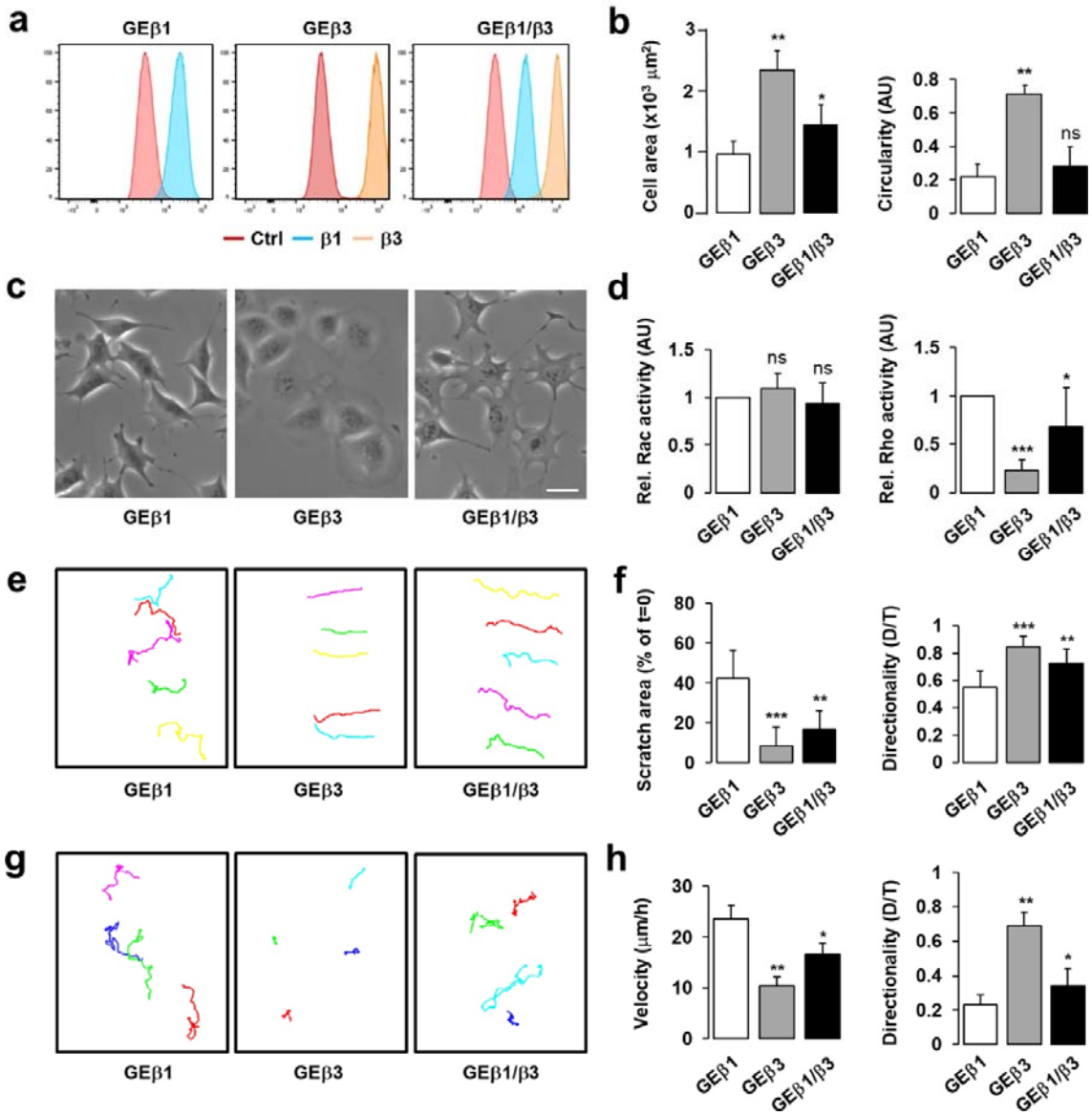

Fig. 1. Reciprocal antagonism between β1 and β3 integrins regulates Rac and Rho activities, cellular phenotype, and cell migration. (a) FACS plots showing cell-surface expression of the human β1 and β3 integrin subunits in GEβ1, GEβ3, and GEβ1/β3 cells. (b) Quantification of cell area (*left*) and 'circularity' (*right*). Values are means + SD from ~150 cells out of 3 independent experiments. (c) Morphology of GEβ1, GEβ3, and GEβ1/β3 cells. Bar, 40 μm. (d) Relative Rac (*left*) and RhoA (*right*) activities in GEβ1, GEβ3, and GEβ1/β3 cells. Values are the means +SD of 3–4 different experiments and normalised to GEβ1 cells. (e) Representative migration tracks of GEβ1, GEβ3, and GEβ1/β3 cells in a scratch assay. The origin is the wound edge at $t = 0$ and direction of migration is from right to left. (f) Scratch closure (*left*) and migration directionality (*right*) of individual cells was determined from scratch assays. Values represent the means +SD from 60 cells out of 3 independent experiments. (g) Representative migration tracks of GEβ1, GEβ3, and GEβ1/β3 cells migrating as single cells. (h) Velocity (*left*) and directionality (*right*) of migrating single cells. Values represent the means +SD from ~60 cells out of 3 independent experiments. Statistically significant differences are indicated by * ($p < 0.05$), ** ($p < 0.01$), and *** ($p < 0.001$). AU; arbitrary units, ns; not significant.

Together, these results show that antagonism between β1 and β3 integrins dictates Rho GTPase activation, cell cohesion, and migratory behaviour.

The β3 cytoplasmic tail regulates cell cohesion and morphology, and balances Rac and RhoA activities in a kindlin-2-dependent manner

We have previously shown that the β1-driven cell scattering and phenotype of GEβ1 cells is prevented by mutations in the β1 cytoplasmic tail [40]. To assess the effect of β3 cytoplasmic tail regions on cellular phenotype, we stably expressed a series of β3 mutants with sequential deletions of the C-terminal domain in GE11 cells: $\beta3^{\Delta759}$ and $\beta3^{\Delta756}$ (truncation within the NITY motif), $\beta3^{\Delta752}$ (truncation in the T/S region), and $\beta3^{\Delta746}$ (truncation within the NPLY motif which is recognised by talin) (Fig. 2a and b). In short-term adhesion assays, all mutant cell lines adhered much less efficiently to FN than GEβ3 cells, confirming the well-established role of both membrane-proximal and membrane-distal cytoplasmic tail regions in cell adhesion (Supplementary Fig. 1b) [41]. Intriguingly, the mutants caused remarkably distinct cellular phenotypes downstream of cell adhesion. While cell spreading decreased progressively with increasing truncation of the β3 tail, truncations within the NITY motif ($\beta3^{\Delta759}$ and $\beta3^{\Delta756}$) also promoted cell-cell dissociation and a dramatic EMT-like morphological change toward a more mesenchymal morphology with many protrusions, in fact supporting a phenotype that strongly resembled that of GEβ1 cells (Fig. 2c and d). Further truncation between the NPLY and NITY motifs (yielding $\beta3^{\Delta752}$) induced only a mild disorganization of cell islands with some protrusions at the edges, while the shortest β3 fragment, truncated within the membrane-proximal NPLY motif ($\beta3^{\Delta746}$), failed to induce any phenotypic changes and cells expressing this mutant formed islands resembling those of the parental GE11 cells (Fig. 2c and d).

We next investigated whether the GEβ1-like phenotype induced by truncation of C-terminal residues, which was most obvious in $GE\beta3^{\Delta759}$ cells, was associated with a difference in the balance of Rac and Rho activities. Interestingly, Rac activity was strongly decreased in $GE\beta3^{\Delta759}$ cells compared to GEβ3, while RhoA activation was concomitantly increased (Fig. 2e; Suppl. Fig. 1c). To further corroborate the role of Rho GTPases in these phenotypes, we transiently expressed Rac and Rho mutants, fused to mCherry to identify positive cells. The $GE\beta3^{\Delta759}$ phenotype could be reversed to that of GEβ3 cells by ectopic expression of constitutively-active Q61L Rac, or dominant-negative T19N RhoA (Fig. 2f). Conversely, expression of dominant-negative N17 Rac into GEβ3 cells induced a protrusive phenotype reminiscent of that of $GE\beta3^{\Delta759}$ cells (Fig. 2g). Because this region is important for kindlin binding [42,43], we investigated whether regulation of the Rac/Rho balance depends on kindlins. Depletion of kindlin-2 (the only kindlin expressed in these cells) in GEβ3 cells induced a strong reduction (up to 70%) in cell adhesion to FN, confirming the well-established role of kindlins in this process (Suppl. Fig. 1d) [18,41]. Strikingly, Rac activation was strongly reduced in kindlin-2-depleted GEβ3 cells, while RhoA activation was concomitantly increased (Fig. 2g).

Taken together, these data show that the C-terminal β3 region regulates the balance between Rac and Rho activities in a kindlin-dependent manner, and functions as a phenotypic switch between epithelial-like cell cohesion versus mesenchymal morphology and cell-cell dissociation.

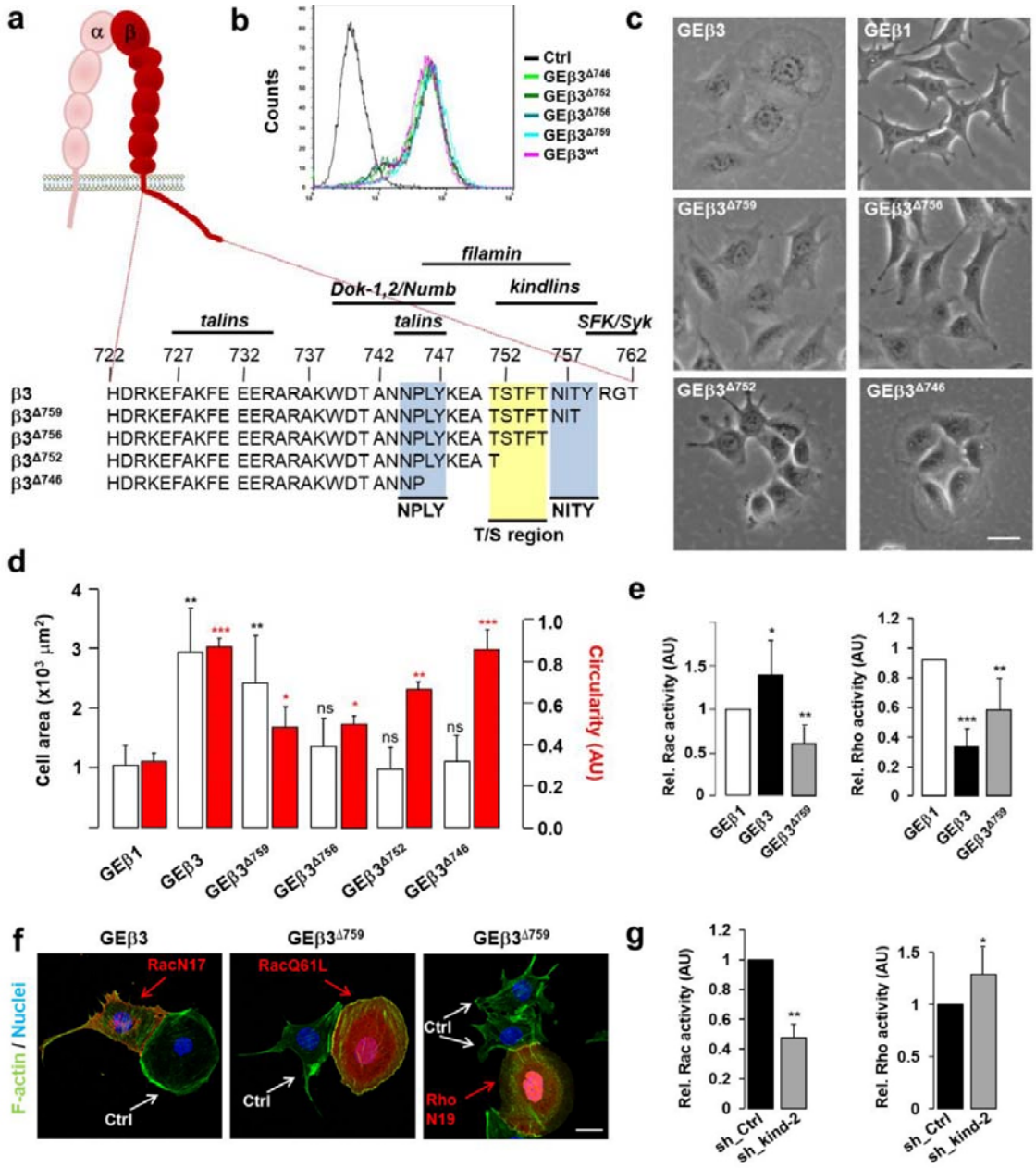

Fig. 2. The kindlin-binding site in β3 is a molecular switch regulating Rac and Rho activities, cellular phenotype, and intercellular adhesion. (a) Amino acid sequences of human wild-type β3 and deletion mutants. Important regulatory motifs such as the T/S region, and the NPLY and NITY motifs are underlined. Known binding sites of proteins that interact with β3 are indicated. (b) FACS plots showing expression of the human β3 subunit on GEβ3, GEβ3$^{\Delta759}$, GEβ3$^{\Delta756}$, GEβ3$^{\Delta752}$, and GEβ3$^{\Delta746}$ cells. (c) Morphology of the indicated cell lines. Bar, 30 µm. (d) Cell area *(white bars*) and 'circularity' (*red bars*), as compared to GEβ1. Values represent the averages +SD of ~200 cells. (e) Relative Rac (*left*) and RhoA (*right*) activities in GEβ3 and GEβ3$^{\Delta759}$ cells, as compared to GEβ1. Values are the means from 3–6 different experiments. (f) GEβ3 and GEβ3$^{\Delta759}$ cells were transiently transfected with the indicated Rac and RhoA constructs, and cells were fixed 24 h later and processed for confocal microscopy. Rac/Rho; red, F-actin; green, nuclei; blue. Bar, 20 µm. (g) Relative Rac (*left*) and RhoA (*right*) activities in GEβ3 cells transduced with shRNAs targeting kindlin-2 (sh_kind-2) or with a non-targeting sequence (sh_Ctrl). Values are the means from 3–6 different experiments. Statistically significant differences are indicated by * ($p < 0.05$), ** ($p < 0.01$), and *** ($p < 0.001$). AU; arbitrary units, ns; not significant.

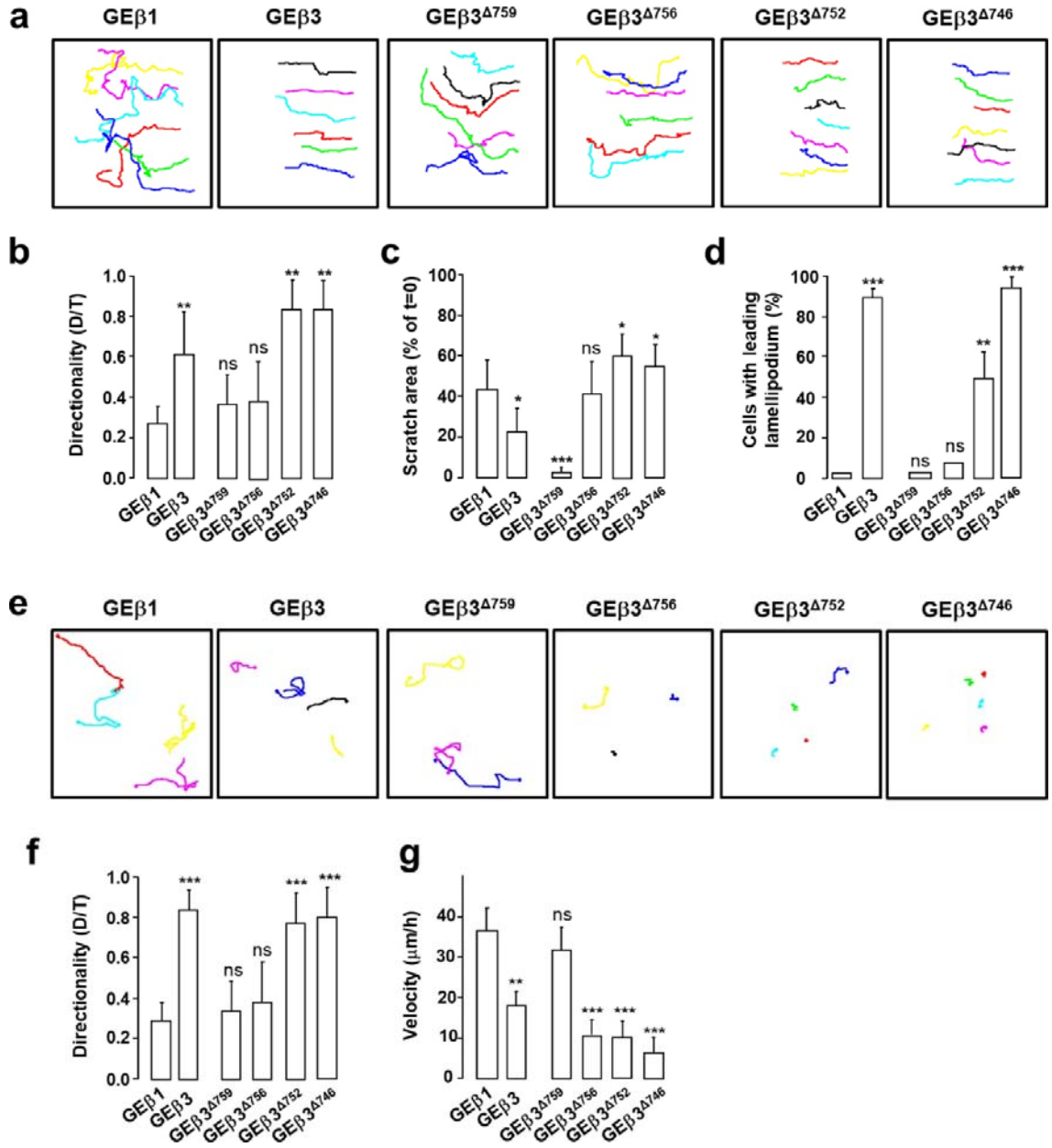

Fig. 3. The kindlin-binding site in β3 regulates collective and directional cell migration versus cell scattering and random cell migration. (a) Representative migration tracks of the indicated cell lines in a scratch assay. The origin is the wound edge at $t = 0$, cells migrate from right to left. (b) The migration directionality of individual cells in scratch assays was quantified for ~100 cells out of 3 experiments. (c) Scratch closure was determined for the indicated cell lines. (d) The mode of cell migration (i.e. broad leading lamellipodium versus multiple thin protrusions) was analysed for ~80 cells out of 3 experiments, and expressed as the percentage of cells that migrated predominantly by means of a leading lamellipodium during 3 h. (e) Representative migration tracks determined in single-cell migration assays. The directionality (f) and average velocity (g) of single-cell migration was determined from ~100 cells out of 3 independent experiments. Values represent the averages +SD. Statistically significant differences are denoted by * ($p < 0.05$), ** ($p < 0.01$), and *** ($p < 0.001$). ns; not significant.

The kindlin-binding region in the integrin β3-tail is a molecular switch regulating migration mode on FN

We next investigated the migratory properties of the generated cell lines in scratch assays. Cells that were poorly cohesive under basal conditions (GEβ1, GEβ3$^{\Delta759}$, and GEβ3$^{\Delta756}$) also lost contact with each other in the scratch assay, generally within three hours after the initiation of migration. Thereafter, they migrated fast and randomly as single cells, not only in the direction of the wound but also parallel to the wound edges (Supplementary Movie 3; Fig. 3a–c). In contrast, GEβ3$^{\Delta752}$ and GEβ3$^{\Delta746}$ cells migrated relatively slowly but in a collective and directional fashion, in line with the integrity of cell-cell contacts under steady-state conditions (Supplementary Movie 3; Fig. 3a–c).

The fast and random cell migration of GEβ1, GEβ3$^{\Delta759}$, and GEβ3$^{\Delta756}$ cells was associated with many rapid cell-shape changes driven by the extension of multiple protrusions that rarely developed into a single, broad lamellipodium, even in cells that were still attached to neighbouring cells (Supplementary Movie 3; Fig. 3d). By contrast, cells that moved collectively and directionally proceeded steadily by means of a stable broad lamellipodium and underwent few shape changes, with GEβ3$^{\Delta752}$ cells displaying a somewhat intermediate phenotype (Supplementary Movie 3; Fig. 3d). The same differences across cell lines were observed in the presence of mitomycin C, indicating that the phenotypes observed in the scratch assays are due to intrinsic differences in cell migration and not proliferation (data not shown). To further confirm this, we also investigated migration of sparsely seeded single cells on FN (5 μg/ml). As observed before, GEβ1 cells were highly motile compared to GEβ3 (Supplementary Movie 4; Fig. 3e–g). Consistent with their phenotype, the migration of GEβ3$^{\Delta759}$ cells was fast and random and resembled that of GEβ1 cells. Strikingly, motility decreased progressively with further truncations of the β3 tail, and GEβ3$^{\Delta752}$ and GEβ3$^{\Delta746}$ cells hardly moved (Supplementary Movie 4; Fig. 3e–g).

In summary, these results demonstrate that the phenotypic switch induced by mutation of the integrin β3 tail is associated with a transition from slow, collective, and directional migration, toward fast and random cell motility.

Cytoplasmic tail mutations in β3 abrogate αvβ3-mediated suppression of β1 integrins

The previous sections have shown that αvβ3 antagonizes β1-dependent RhoA activation and cell-cell dissociation, and that disruption of the kindlin-binding region in β3 causes a switch toward a 'β1-like' phenotype even in the absence of β1 integrins. We next investigated the behaviour of the β3 mutants in the presence of β1 integrins. For this purpose we expressed the β3 mutants into GEβ1 cells, sorted double-positive cells for equal expression levels of β3 by FACS (Fig. 4a), and seeded the resultant cell lines onto FN. Intriguingly, the morphology of all cell lines approached that of GEβ1 cells, indicating that the presence of β1 neutralizes the differences between the β3 mutants (Fig. 4b and c). Indeed, all cell lines were equally dispersed and extended multiple protrusions in all directions, leading to comparable 'circularity' (Fig. 4b and c). Furthermore, cell spreading was similar for all cell lines (Fig. 4b and c). To test whether β1 also smoothed the different migratory phenotypes induced by the β3 mutants, we assessed single-cell migration on FN (5 μg/ml). The presence of β1 integrins hardly affected the already highly migratory phenotype of GEβ3$^{\Delta759}$ cells, but induced high motility in the others, which was most obvious for the otherwise largely stationary GEβ3$^{\Delta752}$ and GEβ3$^{\Delta746}$ mutants (Supplementary Movie 5). Indeed, consistent with the observed cell

morphologies, velocity and directionality were largely similar between all cell lines and approached that of GEβ1/β3 cells (Supplementary Movie 5; Fig. 4d–f).

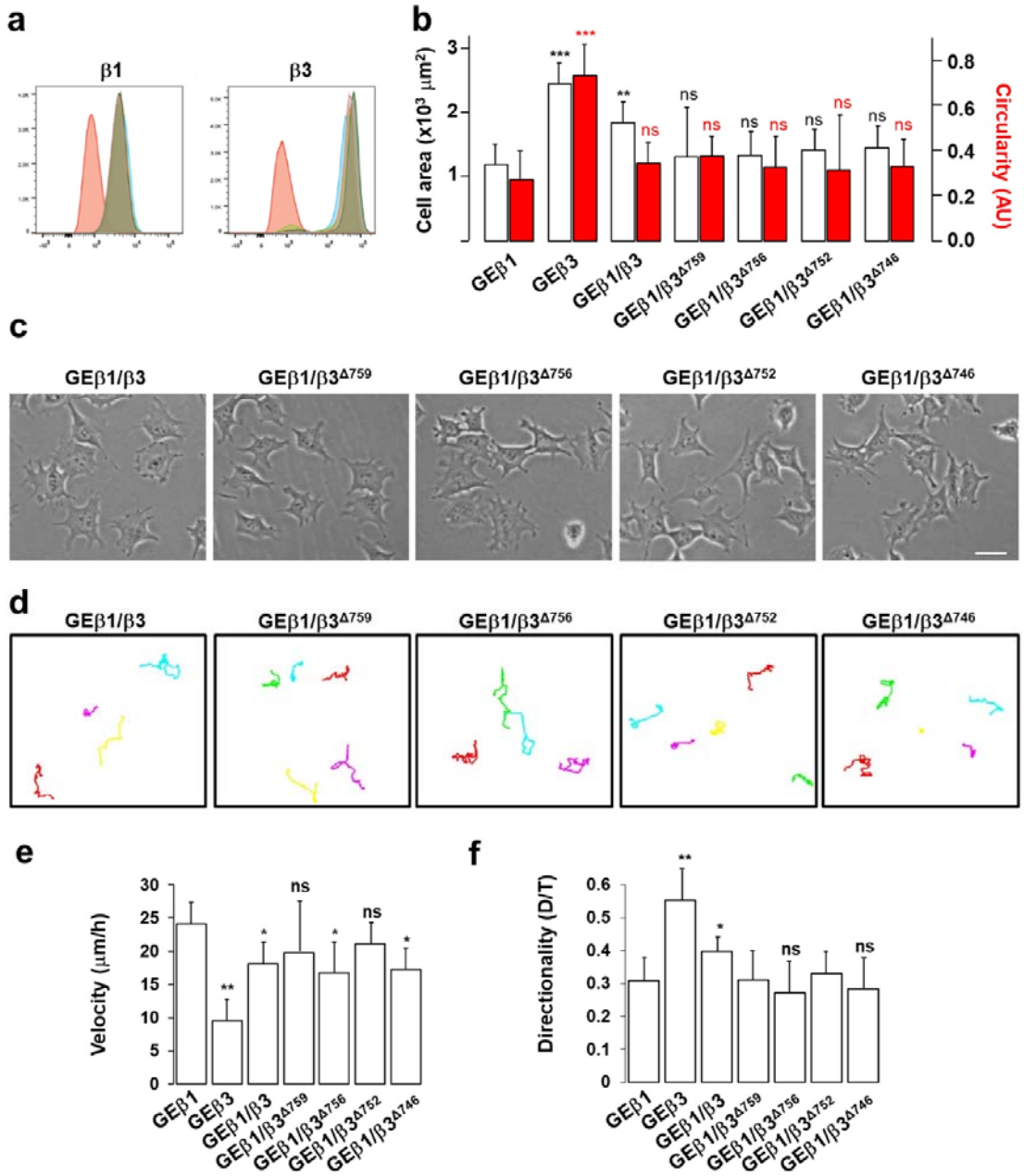

Fig. 4. Cytoplasmic tail mutations abrogate β3-mediated suppression of β1 integrins. (a) FACS plots showing the expression of the human β1 (*left*) and β3 (*right*) integrin subunits in GEβ1/β3, GEβ1/β3$^{\Delta759}$, GEβ1/β3$^{\Delta756}$, GEβ1/β3$^{\Delta752}$, and GEβ1/β3$^{\Delta746}$ cells. (b) Quantification of cell area (*white bars*) and 'circularity' (*red bars*) for the indicated cell lines. Values are means + SD from ~150 cells out of 3 independent experiments. (c) Morphology of the indicated cell lines on FN (5 μg/ml). Bar, 20 μm. (d) Representative migration tracks determined in single-cell migration assays. The average velocity (e) and directionality (f) of single-cell migration was quantified for ~100 cells out of 3 experiments. Values represent the averages +SD. Statistically significant differences are denoted by * ($p < 0.05$), ** ($p < 0.01$), and *** ($p < 0.001$). AU; arbitrary units, ns; not significant.

Taken together, these data show that αvβ3 requires the kindlin-binding region to antagonize β1 integrin-dependent effects on cell morphology, dissociation, and migration. Furthermore, integrin β1 is dominant over the β3 cytoplasmic tail mutants, and overrules their differential effects on cell cohesion, morphology, and migration.

Antagonism between β1 integrins and αvβ3 regulates endothelial cell morphology, Rho GTPase activation, and monolayer integrity

The previous sections have shown that reciprocal suppression by β1 integrins and αvβ3 regulates cell cohesion, Rho GTPase activation, and migratory properties in murine neuro-epithelial GEβ1/β3 cells. To further strengthen these observations in a relevant human cell system, we selectively depleted β1 or β3 in primary human umbilical vein endothelial cells (HUVECs) using short hairpin RNAs (shRNAs) (Fig. 5a). In line with our observations in GEβ1/β3 cells, knockdown of β1 expression strongly increased cell spreading in HUVECs, whereas depletion of β3 reduced it (Fig. 5b; Suppl. Fig. 2a; Suppl. Fig. 3c). These effects were observed both for sparsely seeded cells as well as cells in monolayers (Fig. 5c and e; Suppl. Fig. 2a). However,it should be noted that in the absence of β1 integrins, HUVEC monolayers also contained fewer cells, possibly due to decreased proliferation (Fig. 5e). Neither β1 nor β3 depletion resulted in a loss of (mainly peripherally located) FAs, as indicated by phosphotyrosine staining, although their distribution seemed different (Fig. 5c). The formation of FBs, which are associated with RhoA activation, was strongly reduced in β1-depleted cells, as assessed using ectopically expressed GFP-tensin-1 as a marker (Fig. 5c). We then examined Rac and Rho activities in HUVEC monolayers that were untreated or treated with thrombin, a potent inducer of RhoA activation. Thrombin-induced RhoA activation and concomitant stress fiber formation lead to the disruption of adherens junctions and cell retraction, a process that induces endothelial permeability and barrier disruption [7,[44], [45], [46], [47]]. This process is counteracted by Rac-dependent cell spreading, thus promoting endothelial barrier recovery [7,[44], [45], [46], [47]]. In line with the observed absence of FBs, β1-depleted cells had significantly lower thrombin-induced RhoA activation than control cells, while β3-depleted HUVECs showed increased RhoA activation (Fig. 5d; Suppl. Fig 2b). In contrast, Rac activation was not significantly different upon depletion of either β1 or β3 (Fig. 5d; Suppl. Fig 2b). The differences in RhoA GTPase activity were paralleled by strong cell retraction in response to thrombin in β3- but not β1-depleted cells, generating large intercellular gaps in the monolayer (Fig. 5e and f).

Collectively, these experiments are in line with our observations in GEβ1/β3 cells and show that in HUVECs, β1 integrins and αvβ3 have counteracting effects on the activity of Rho GTPases, cell spreading and contraction, and the stability of cell-cell adhesion.

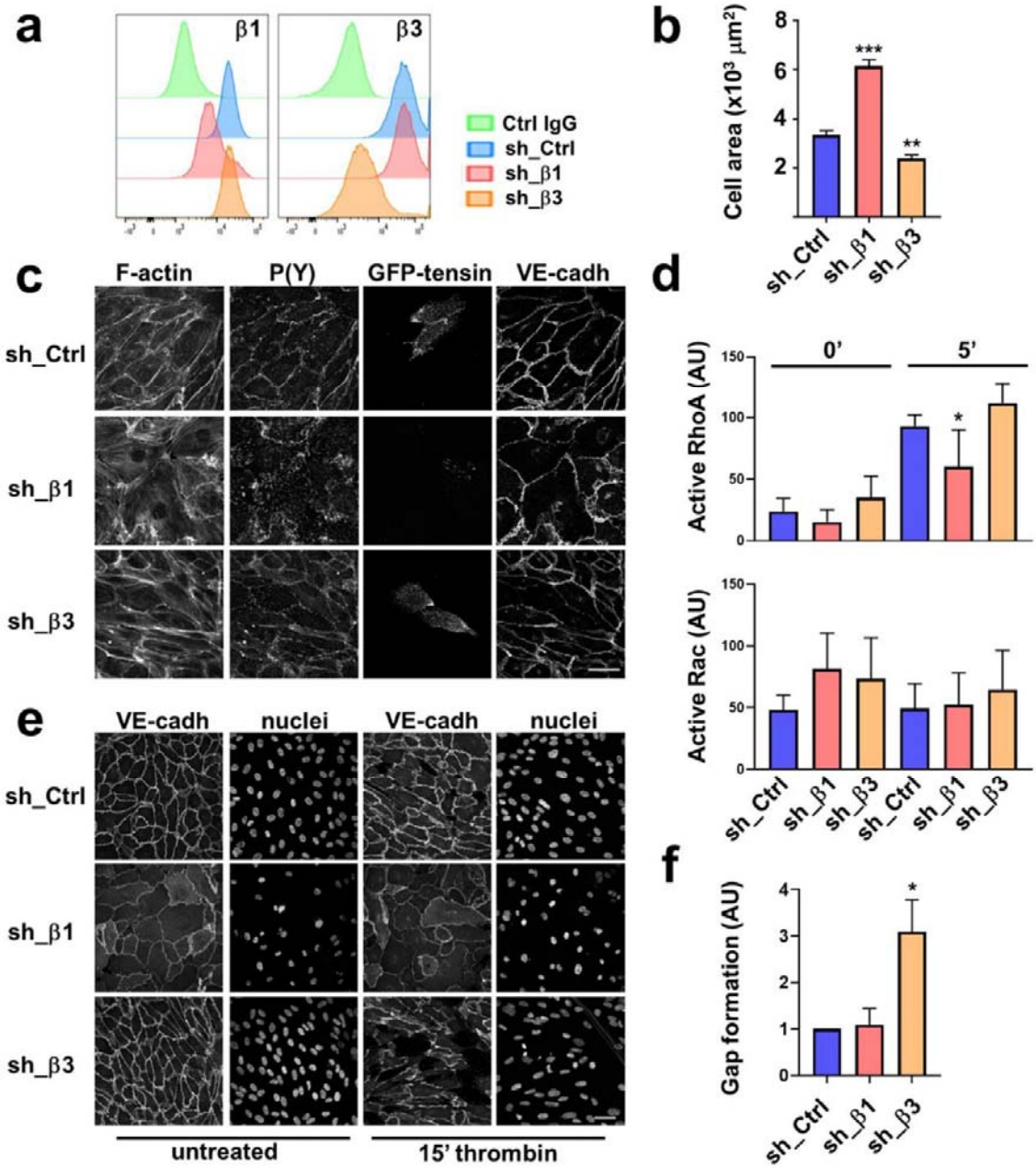

Fig. 5. Antagonism between β1 and β3 integrins regulates cell morphology, Rac and Rho activities, and monolayer integrity in endothelial cells. (a) FACS plots showing the expression of β1 and β3 integrins on HUVECs transduced with non-targeting sequences (sh_Ctrl) or with shRNAs against β1 or β3. (b) Quantification of cell area. Values are means +SD from 117 to 175 sparsely seeded cells out of 3 independent experiments. (c) Confocal images of sh_Ctrl, sh_β1, and sh_β3 HUVEC monolayers showing F-actin, phosphotyrosines, GFP-tensin-1, and VE-cadherin. Bar, 20 μm. (d) Relative Rac and RhoA activities in sh_Ctrl, sh_β1, and sh_β3 HUVEC monolayers, untreated or treated for the indicated time-points with thrombin (1 U/ml). (e) Confocal images of VE-cadherin (*left panels*) and nuclei (*right panels*) in HUVEC monolayers, either untreated or incubated with thrombin for 15 mins. (f) Quantification of thombin-induced gap formation. Values represent the averages +SD of 3 experiments. Bar, 50 μm. Statistically significant differences are denoted by * ($p < 0.05$), ** ($p < 0.01$), and *** ($p < 0.001$). AU; arbitrary units, P(Y); phosphotyrosines, VE-cadh; VE-cadherin.

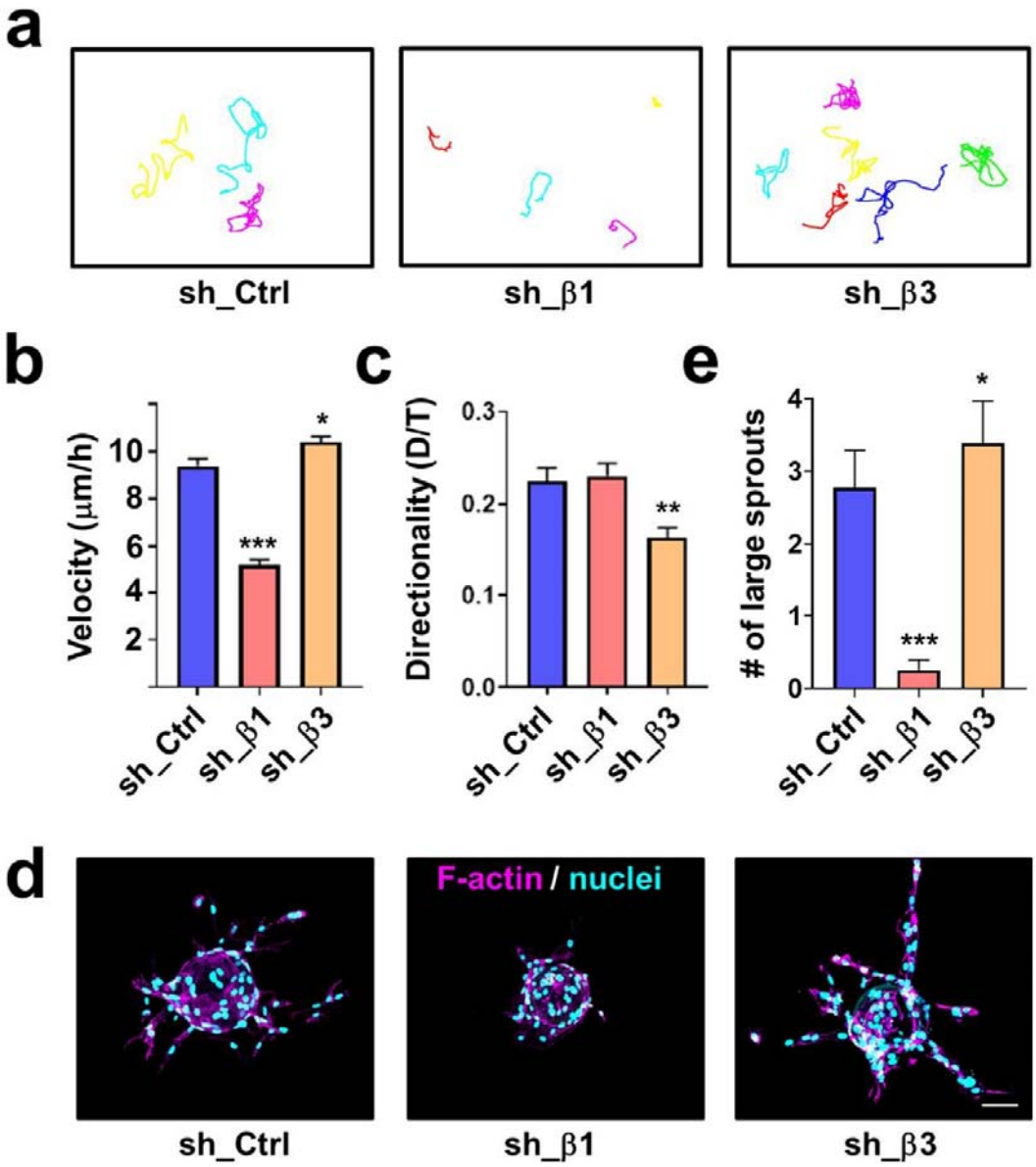

Fig. 6. Antagonism between β1 and β3 integrins regulates cell migration and angiogenic sprouting in endothelial cells. (a) Representative single-cell migration tracks of sh_Ctrl, sh_ β1, and sh_β3 HUVECs on FN (5 μg/ml). Velocity (b) and directionality (c) of single-cell migration. Values represent the means +SD from 132 to 175 cells out of 3 independent experiments. (d) Maximum projections of confocal z-stacks showing HUVEC sprouting from collagen-coated beads into fibrin gels. z-stacks were recorded 48 h after growth factor addition. Bar, 100 μm. (e) Sprouting was scored as the number of 'large sprouts' (> than the bead diameter)/bead. Values represent the averages +SD from ~60 beads per condition, pooled from 3 independent experiments. Statistically significant differences are indicated by * ($p < 0.05$), ** ($p < 0.01$), and *** ($p < 0.001$). Ctrl; control.

Integrin antagonism in endothelial cells regulates cell migration and sprouting angiogenesis

We next assessed how β1/β3 crosstalk affects single-cell migration in HUVECs on FN (5 μg/ml). While the knockdown of β1 expression clearly decreased the migration velocity of HUVECs, depletion of β3 caused the opposite effect (Fig. 6a and b; Suppl. Fig. 3). In addition, the directionality of cell migration was reduced by β3 knockdown (Fig. 6c; Suppl.

Fig. 3). As a model for collective endothelial cell migration, we also investigated β1/αvβ3 integrin crosstalk in vascular endothelial growth factor (VEGF)-induced sprouting angiogenesis in fibrin gels [48]. Interestingly, HUVECs depleted of β1 integrins completely failed to sprout, while sprouting was modestly increased in β3-depleted HUVECs (Fig. 6d and e).

Together, our findings show that β1/αvβ3 antagonism regulates migratory behaviour in endothelial cells, both on FN-coated two-dimensional surfaces and in three-dimensional fibrin environments.

Antagonism between β1 integrins and αvβ3 regulates cellular phenotype, Rho GTPase activities, and cell migration in human trophoblasts

Finally, we wished to confirm β1/β3 antagonism in another human cell system, for which we chose human trophoblasts, epithelial cells derived from the fetus that invade into the uterine wall during placenta development [49]. As a model system we used the human first-trimester trophoblast cell line HTR8/SVneo[50], which expresses both β1 and β3 (Fig. 7a). Depletion of β1 or β3 caused essentially the same phenotypical differences as in HUVECs; cell spreading was increased by knockdown of β1 expression, while the opposite was observed for β3-depleted cells (Fig. 7a and b). Furthermore, β1 depletion caused decreased RhoA activation in response to thrombin, while in β3-depleted cells higher levels of active RhoA were found (Fig. 7c). In contrast, Rac activation was significantly reduced by knockdown of β3, but not of β1 (Fig. 7c). Finally, we assessed cell migration in scratch assays. Also here, depletion of β1 and β3 had opposite effects, in line with the observed role of these integrins in HUVECs and GEβ1/β3 cells. Knockdown of β1 slowed down cell migration, while β3 depletion induced faster migration but a loss of directional persistence (Fig. 7d–g).

Together, these results confirm that in human placental trophoblasts, reciprocal antagonism between β1 and β3 integrins regulates cellular phenotype, activation of Rho GTPases, and migratory behaviour.

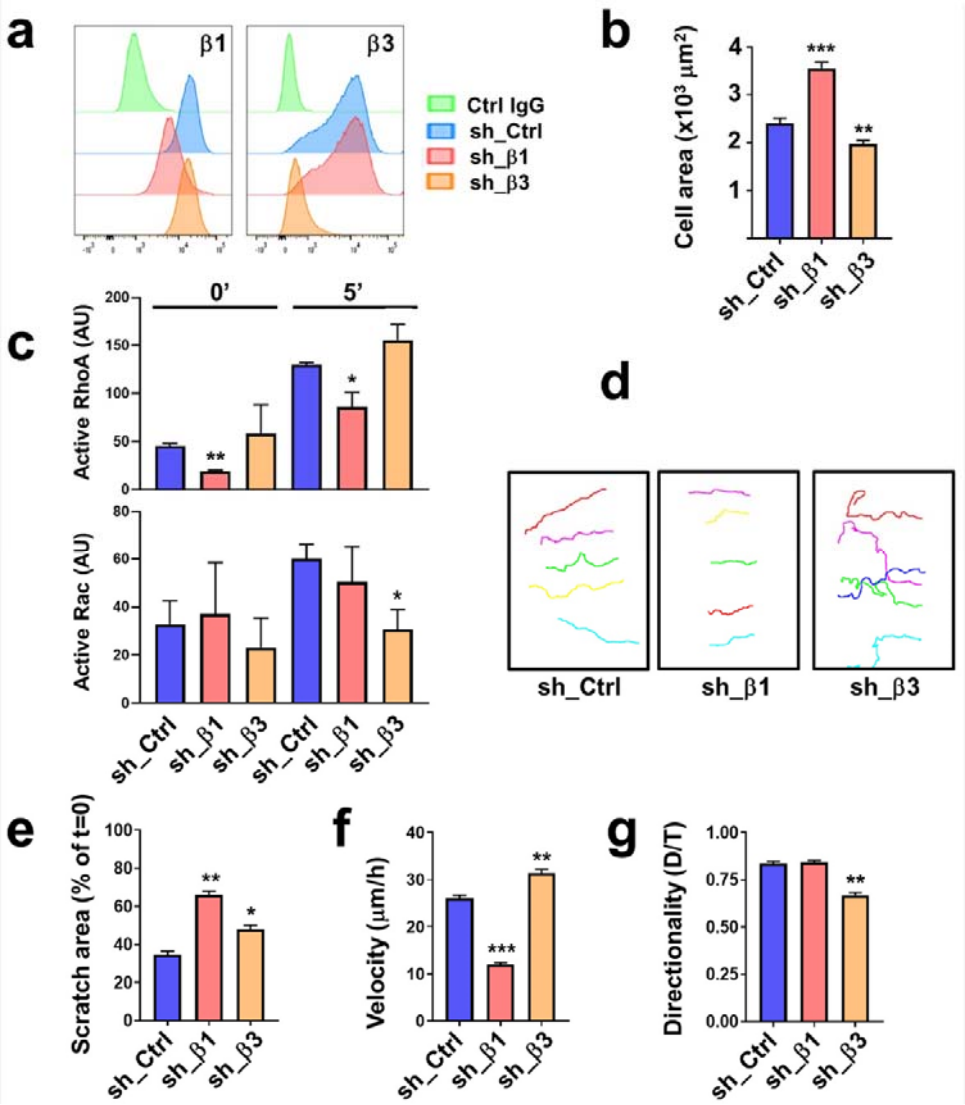

Fig. 7. Antagonism between β1 and β3 integrins regulates Rac and Rho activities, cell morphology, and cell migration in human trophoblasts. (a) FACS plots showing the expression of β1 and β3 integrins on HTR8 trophoblasts transduced with non-targeting sequences (sh_Ctrl), or with shRNAs against β1 or β3. (b) Quantification of cell area. Values are means +SD from 76–91 cells out of 3 independent experiments. (c) Relative Rac and RhoA activities in sh_Ctrl, sh_β1, and sh_β3 HTR8 trophoblasts, either untreated or incubated for 5 min with thrombin (1 U/ml). (d) Representative migration tracks of sh_Ctrl, sh_β1, and sh_β3 HTR8 trophoblasts in a scratch assay. The origin is the wound edge at $t = 0$ and the direction of migration is from right to left. Scratch closure (e), velocity (f), and migration directionality (g) were determined from 3 independent experiments. Values represent the means +SD from 75 cells out of 3 independent experiments. Statistically significant differences are indicated by * ($p < 0.05$), ** ($p < 0.01$), and *** ($p < 0.001$). Ctrl; control.

Discussion

In this study, we show that RGD-binding β1 and β3 integrins induce very distinct cellular phenotypes in a reciprocally antagonistic manner, which regulate intercellular adhesion and cell migration in trophoblastic, neuro-epithelial, and endothelial cells. While β1 integrins attenuate β3-dependent cell spreading, β3 integrins counteract β1-induced RhoA activation and cell contractility. The β3 integrin-regulated balance between Rac and RhoA activities is abolished by cytoplasmic tail mutations that disrupt the kindlin-2-binding site (comprising

the NITY motif and the T/S region), causing a loss of cell cohesion and directional cell migration. Remarkably, this results in a phenotypic switch toward a 'β1-like' mesenchymal phenotype, even in the absence of β1 integrins. It is noteworthy that further truncation of the β3 tail within the membrane-proximal NPLY motif leads to a loss-of-function, probably because this mutation also compromises the binding of talin, in addition to that of kindlin-2. Consistent with the phenotypes of the kindlin-binding mutants, a dysregulation of Rac and RhoA activities was also observed upon kindlin-2 depletion. Together, these findings imply that kindlin-2 regulates isotropic cell spreading and cell-cell adhesion by controlling the balance between Rac and RhoA activities. This hypothesis is supported by the observations that kindlin-2 binds paxillin to activate Rac1, and associates with the Arp2/3 complex to induce Rac1-mediated membrane protrusions [51,52]. Furthermore, kindlin deficiency promotes RhoA activity [53], and compromises epithelial and endothelial barrier function [54,55]. Finally, kindlin-2 recruits the integrin-linked kinase/parvin/PINCH complex to integrins [56,57]. Disruption of this complex in endothelial cells causes a loss of Rac activation and an increase in RhoA, resulting in a switch to a hyper-contractile phenotype associated with random instead of directional cell migration, thus strongly resembling our findings [57]. In addition to kindlins, other proteins that bind integrin β-tails at approximately the same binding site (Fig. 2a) may also regulate Rac and Rho activity, such as filamins. Intriguingly, filamin A has been shown to recruit two different GTPase-activating proteins for Rac to β1 integrins, thus downregulating Rac activity at adhesion sites [58,59].

Our data confirm the well-accepted view that the balance between relative activities of different Rho GTPases is critical for migratory behaviour [4,5,[9], [10], [11], [12], [13], [14],58,60], and show in addition that specific integrins can trans-dominantly inhibit each other's function through differential effects on Rho activation. Because the β3 mutants can no longer suppress the β1-associated phenotype but instead are 'overruled' by wild-type β1, antagonism depends on sequences in the cytoplasmic tail. Intriguingly, earlier studies have reported that ligation of integrins can trans-dominantly inhibit the activation of others through sequestration of talin [61], [62], [63]. Trans-dominant effects through cytoplasmic tail sequences extend the cell's repertoire for differential integrin use, in addition to differential interactions of distinct integrins with the same ligand. While αvβ3 binds only the RGD site in FN, α5β1 binds both the RGD and the synergy site, leading to high-affinity binding and efficient assembly of FN into fibrils [64], [65], [66]. Previous work from us and others in different cell types has shown that α5β1 is the predominant FN-binding β1 integrin responsible for the phenotype described here, consisting of RhoA activation, FN fibrillogenesis, cell scattering, and fast cell migration [30,37,38,67]. Other β1 integrins can recognize FN as well, including αvβ1 and α8β1 (which recognize the RGD), and α4β1 and α9β1 (which bind the LDV motif). Importantly, the tissue distribution of these integrins is more restricted than that of α5β1, and they also interact with a variety of other matrix proteins besides FN. Indeed, the phenotypes of knockout mice lacking their respective α-subunits reveal very specific in vivo functions for these integrins that are mostly mediated by interactions with other proteins than FN. For instance, α9β1 binds tenascin and EMILIN and is required for the development of lymphatic valves and lymphangiogenesis, α8β1 promotes kidney development through interactions with nephronectin, and α4β1 interactions with vascular cell adhesion molecule-1 mediate leukocyte trafficking as well as cardiac and placental development [68], [69], [70], [71], [72]. In contrast, α5-null mice die early during embryonic development [73]. Finally, it will be important to determine the function of αvβ1. This integrin plays a crucial role in tissue fibrosis through activation of transforming growth factor-β [74]. However, since both the αv and β1 subunits are part of several heterodimers,

studying αvβ1 is complicated and virtually nothing is known about the responses it induces downstream of FN.

Reciprocal inhibition of β1 and β3 integrins may be an important feedback mechanism to limit integrin function in pathophysiological conditions where extensive cell migration, morphogenesis, and tissue remodeling occur. Migrating cell cohorts express α5β1 and αvβ3 during placental invasion and embryonic development, sprouting angiogenesis, and in wounds and tumors, often in a spatiotemporally restricted manner. In many of these processes, transient differences in integrin expression and/or function may regulate cellular plasticity, cell cohesion versus cell dissociation, and thus collective versus individual cell migration. For example, migrating neural crest cells express αvβ3 and several β1 integrins, of which mainly α5β1 is crucial for neural crest morphogenesis [75], [76], [77], [78], [79]. The onset of α5β1 expression is associated with activation of RhoA, the loss of cell-cell adhesion and EMT, and a switch from collective to individual cell migration [80,81]. Intriguingly, excessive RhoA/ROCK activation due to exaggerated β1 integrin signaling disrupts neural crest cell targeting to their final destinations, underlining that efficient neural crest morphogenesis requires antagonism of β1 integrin-dependent RhoA activation and cytoskeletal contractility [81].

Integrin αvβ3 is also strongly expressed on activated endothelial cells during sprouting angiogenesis, where it forms a functional complex with VEGFR2 and enhances VEGF-induced signaling and cell migration [82], [83], [84]. Whereas inhibition of αvβ3 using small molecules or blocking antibodies induces angiogenic defects in a variety of systems, β3-null mice display no apparent defects in developmental angiogenesis, and even have increased angiogenesis in tumors [85,86]. The latter is due to strongly increased VEGFR2 expression in the absence of β3 [85]. We observed a slight increase in sprouting upon β3 depletion, but no upregulation of VEGFR2 expression (data not shown). In light of our data, we reason that αvβ3 inhibits β1-dependent endothelial sprouting through its cytoplasmic tail domains and that therefore, knockdown of β3 produces effects that are different from blockade of the extracellular domain, which still leaves signaling through the cytoplasmic tail intact. Thus, the role of αvβ3, and possibly other αv integrins as well, in angiogenesis may depend at least in part on reciprocal crosstalk with β1 integrins. This scenario is supported by the phenotypes of integrin knockout mice in developmental angiogenesis; although there is redundancy to some extent between α5β1 and αv integrins, excessive angiogenesis is observed in the absence of the latter, which is nullified by the loss of α5β1 [87,88].

Finally, the regulation of intercellular adhesion by reciprocal β1/β3 integrin antagonism may prove very important for several clinical conditions related to endothelial dysfunction. Disruption of the endothelial barrier during injury or inflammation can occur by a variety of agents including thrombin, histamine, inflammatory cytokines, and lipopolysaccharide (LPS), and involves Rho-dependent disruption of VE-cadherin-based intercellular junctions [15,16,[44], [45], [46], [47]]. Importantly, barrier disruption is counteracted by Rac-dependent cell spreading and the re-establishment of cell-cell contacts by VE-cadherin, which prevents life-threatening complications resulting from excessive leakage [15,16,[44], [45], [46], [47]]. Our data show that the differential regulation of Rho and Rac activities by β1 and β3 integrins regulates endothelial monolayer integrity, and suggest that αvβ3 strengthens endothelial barrier function, while β1 integrins promote barrier disruption. These findings are in line with the observations that inflammation-induced vascular leakage by challenge with LPS is enhanced in β3-null mice, and that blocking antibodies against αvβ3 enhanced permeability of endothelial monolayers in vitro in response to a variety of barrier-disruptive

agents [89]. Moreover, activation of endothelial β1 integrins induces barrier disruption, while blocking antibodies against β1 integrins protect from LPS-induced barrier disruption and vascular leakage in mice [90,91].

Altogether, integrin antagonism may be an important regulatory mechanism in a variety of pathophysiological contexts to control dynamic collective cell processes, including cell migration and tissue remodeling.

Experimental procedures

Antibodies, plasmids and other materials

Antibodies used were directed against β-actin (clone C4; Chemicon), integrin β3 (clone C-17 from Dr. E. van der Schoot, Sanquin Research, Amsterdam, The Netherlands; integrin β1 (clone TS2/16, Developmental Studies Hybridoma Bank), kindlin-2 (from Dr. R. Faessler, Max Planck Institute of Biochemistry, Martinsried, Germany), P(Y) (clone 4G10 from Sigma-Aldrich), Rac (Transduction laboratories), RhoA (Cell Signaling), VE-Cadherin (clone 55-7H1, BD biosciences) and VEGFR2 (R&D Systems). The β3 deletion mutants were obtained from Dr. J. Ylanne (University of Jyvaskyla, Finland) and recloned into LZRS-IRES-zeo as described previously [92], while Rac and RhoA mutants fused to mCherry or GFP were from Dr. J. Collard (Netherlands Cancer Institute, Amsterdam, The Netherlands). GFP-tensin-1 was from Dr. K. Yamada (National Institute of Health, Bethesda, MD), Rhotekin-RBD and PAK-CRIB peptides were home-made, human fibrinogen was from CSL Behring, collagen-coated Cytodex beads, puromycin, zeocin, human thrombin, and human FN were from Sigma-Aldrich. TRITC-, FITC-, and Cy5-conjugated secondary antibodies, phalloidins, and DAPI were from Molecular Probes, Fugene was from Promega, and HRP-conjugated secondary antibodies were from Amersham.

Cell culture, transient transfections, and retroviral transductions

Human embryonic kidney (HEK) 293T cells and ecotropic Phoenix packaging cells (both obtained from ATCC) and GEβ1/β3 cells were maintained in Dulbecco's modified Eagle medium (DMEM) (Thermo Fisher Scientific) containing 4.5 g/L D-glucose, L-glutamine, 10% (v/v) FCS (Bodinco), 1 mM sodium pyruvate (Thermo Fisher Scientific), and 1 U/ml penicillin/streptomycin. Pooled HUVECs from up to 5 individual donors were purchased from Lonza and cultured in endothelial basal medium-2 (Bio-Connect Life Sciences) containing growth supplements (Bio-Connect), 200 mM l-glutamine (Sigma-Aldrich), and 1 U/ml penicillin/streptomycin (Sigma-Aldrich). HUVECs were used between passages 3 and 6 and routinely passaged on cell culture flasks coated with 0.1% gelatin (Sigma-Aldrich). HTR-8/SVneo cells were obtained from ATCC and cultured in RPMI supplemented with 5% FCS, and 1 U/ml penicillin and streptomycin. All cells were maintained at 37 °C in a humidified atmosphere containing 5% CO_2. Constructs encoding wild-type or mutant integrins were transfected into Phoenix packaging cells using the Calcium Phosphate method. Virus-containing supernatant was isolated 48 h later and stable expression in GE11 cells was achieved by retroviral transduction, followed by selection with zeocin (200 µg/ml) and FACS. Transient transfections were performed either using Fugene or by electroporation using the Amaxa nucleofector as described previously [40].

Lentiviral transduction and RNA interference

ShRNAs cloned into pLKO.1 were obtained from the TRC Mission library and included: (TRCN0000) 191,859, 190,504, and 191,858 (against mouse kindlin-2); 275,134, 275,133, 275,083, 275,135, and 275,082 (against human integrin β1); and 003,236, 003,235, and 003,237 (against human integrin β3). To produce lentiviral particles containing shRNAs, HEK 293T cells were transfected using *Trans*IT-LT1 transfection reagent (Mirus Bio) according to the manufacturer's protocol. Supernatant was harvested 48 and 72 h after transfection, centrifuged, filtered over a 0.45 µm pore filter, aliquoted and stored at −80 °C. Cells were lentivirally transduced with individual or pooled shRNAs, while a scrambled sequence in pLKO.1 was used as a control. Positive cells were selected during 3 days using 1 µg/ml (HUVECs and HTR8) or 5 µg/ml (GE cells) puromycin (Sigma-Aldrich). Similar results were obtained with different shRNAs (Suppl Figs. 1 and 3, and data not shown).

Flow cytometry and cell sorting

For flow cytometry and cell sorting, trypsinised cells were washed twice in PBS containing 2% FCS, and incubated with primary antibodies for 45 min at 4 °C. Cells were then washed twice in 2% FCS/PBS, incubated with appropriate secondary antibodies for 45 min at 4 °C, washed twice in 2% FCS/PBS, and analyzed on a FACS Calibur (BD Biosciences). Alternatively, the cells were sorted on a MoFlo High Speed Cell Sorter (Beckman Coulter).

Cell lysis and western blotting

Cells were washed in ice-cold PBS and lysed on ice in RIPA buffer (25 mM Tris/HCl pH 7.6, 150 mM NaCl, 1% NP-40, 0.5% sodium deoxycholate, 0.1% SDS), supplemented with protease inhibitor cocktail (Sigma-Aldrich). Cell lysates were centrifuged at 13,000x*g*, heated at 95 °C in SDS sample buffer (50 mM Tris–HCl pH 6.8, 2% SDS, 10% glycerol, 1% β-mercaptoethanol, 12.5 mM EDTA, 0.02% bromophenol blue), and proteins were resolved by SDS-PAGE, after which they were transferred to polyvinylidene difluoride membranes (Millipore) and analyzed by Western blotting as described previously [40,93], followed by ECL using the SuperSignal system (Pierce Chemical Co.).

Rac and RhoA activity assays

Rac and Rho assays were performed as previously described [94]. Briefly, cells were seeded in 10 cm dishes coated with FN (5 µg/ml) at 70–80% confluency. HUVECs and HTR8/SVneo cells were stimulated with thrombin (1 U/ml in serum-free medium) the next day for the indicated time-points and then lysed, while GE-derived cell lines were lysed 3 h after seeding. For GEβ3 cells in which kindlin-2 was depleted, non-adherent cells were collected from the medium by centrifugation and pooled with the adherent fraction in lysis buffer. All cells were washed with ice-cold PBS prior to lysis in buffer containing 25 mM Tris–HCl pH 7.2, 150 mM NaCl, 10 mM $MgCl_2$, 1% NP-40, 5% glycerol, and protease inhibitors. Lysates were centrifuged for 5 min, 14000x*g* at 4 °C, and incubated with bacterially produced GST-Rhotekin-RBD beads (RhoA activation assay) for ≥1 h at 4 °C. After incubation, samples were centrifuged for 20 s, 5000x*g* at 4 °C, GST-Rhotekin-RBD beads were placed on ice, and supernatants were incubated for 30 min with 30 µg of a biotinylated PAK1-CRIB peptide (Rac activation assay) coupled to streptavidin agarose beads. Subsequently, all beads were washed 5 times with lysis buffer, boiled in SDS sample buffer, and analyzed by Western blotting. Bands of pulldowns as well as total cell lysates were quantified by densitometry using Fiji/ImageJ. Results are expressed as the ratio active GTPase/total GTPase.

Microscopy

Phase-contrast images were acquired on a Zeiss microscope (Axiovert 25) at 10x (NA 0.25) or 20x (NA 0.3) magnification, using a Zeiss CCD camera (Axiocam MRC) and Zeiss Mr. Grab 1.0 software. Quantification of cell area and circularity was performed using Fiji/ImageJ (version 1.52e).

For confocal microscopy of fixed cells, cells were prepared on coverslips as previously described [39], and images were acquired on an inverted confocal microscope (Leica AOBS or SP8) using 20x (NA 0.7) dry, 40x (NA 1.25) oil, and 63x (NA 1.32) oil objectives (Leica). Images were processed using Leica Application Suite X and Fiji/ImageJ (version 1.52e) software.

For confocal microscopy of sprouting assays, fibrin gels with beads were permeabilized for 5 mins in 0.5% Triton X-100, and blocked in 5% BSA in PBS containing 1 mM CaCl2 and 0.5 mM MgCl2 for 2 h at RT. Afterwards the gels were washed 3 times with PBS++ and DAPI and phalloidin were incubated overnight at 4 °C. The following day the gels were washed 3 times with PBS++ for 10 min. The beads were visualized using a 25x long-distance water objective on a Leica SP5 confocal microscope, creating z-stacks of 1.5 µm per slice, resulting in 150–200 slices per bead. A maximum projection of the image stacks was created using Fiji/ImageJ.

Cell adhesion and migration assays

For adhesion assays, 96-well plates were coated with FN, washed with PBS, and blocked with 2% BSA. Cells were seeded at a density of 3×10^4 per well in DMEM w/o FCS. After 30 min at 37 °C, non-adherent cells were washed away with PBS. Remaining cells were fixed in 4% PFA, washed with H2O, stained with crystal violet, washed, and lysed in 2% SDS. Absorbance was measured at 590 nm.

For scratch assays, cells were grown to confluency, serum-starved overnight, and 10 µg/ml Mitomycin C (Nycomed Inc.) was added 2 h prior to scratching with a pipette tip. After 2 washings with serum-free medium, cells were stimulated with FCS-containing medium. Phase-contrast images were captured every 10 min at 37 °C and 5% CO_2 on a Widefield CCD system using a 10x dry lens objective (Carl Zeiss MicroImaging, Inc.). Images were processed and scratch areas were analyzed using Fiji/ImageJ. Scratch closure is represented as the ratio of the wound area after overnight migration over the wound area at $t = 0$. Values shown represent the means +SD of 3 independent experiments. Individual cell migration tracks were generated using Fiji/ImageJ, and the directionality of cell migration was determined as described previously [40,93]. The percentage of cells that displayed 'lamellipodial migration' was determined from time-lapse movies and expressed as the number of cells that maintained a stable leading lamellipodium during 3 h.

For single-cell migration assays, cells were sparsely seeded on 5 µg/ml FN, and phase-contrast images were captured every 10 min during 18 h at 37 °C and 5% CO_2 on a Widefield CCD system using a 10x dry lens objective (Carl Zeiss MicroImaging). Migration tracks were generated using Fiji/ImageJ, and the average velocity was calculated from 60 to 150 cells out of 3 independent experiments.

Quantification of endothelial monolayer integrity

Confluent monolayers on coverslips were either left untreated or stimulated with thrombin (1 U/ml) for the indicated time. Thereafter, the cells were fixed with 4% PFA and processed for confocal microscopy as described above using DAPI, phalloidin, and anti-VE-cadherin. Tile-scans of coverslips were then acquired on a Leica confocal SP8 using the 20x objective. Images consisting of stitched tiles were then color-inverted, thresholded, and the open areas were quantified using Fiji/ImageJ.

Sprouting assays

Sprouting assays were performed according to previously established protocols with minor modifications [48]. In brief, HUVECs were incubated with collagen-coated microcarrier beads (Sigma-Aldrich). The next day, the beads were detached by washing and transferred to 48-well plates containing fibrinogen in PBS (2 mg/ml) with 6.25 U/ml thrombin. EGM-2 medium with or without integrin-blocking antibodies was added on top of the gels. Beads were imaged by time-lapse microscopy on a Widefield system using a 10x dry lens objective (Carl Zeiss MicroImaging, Inc.). Images were recorded at 15-min intervals during 48 h. For each condition, 20 beads were analyzed per experiment. Sprouting was assessed as the average number of large (length of sprout > the bead diameter) sprouts per bead. Alternatively, beads were embedded in fibrin gels in 'half-area' glass-bottom 96-well imaging plates (Corning). After 48 h, beads were fixed, stained with DAPI and phalloidin, and visualized by generating z-stacks on a confocal microscope.

Statistical analysis

Statistical analysis was performed using one-way ANOVA for multiple comparisons and unpaired *t*-tests for comparisons between two conditions. Throughout the paper, statistically significant differences are indicated by * ($p < 0.05$), ** ($p < 0.01$), *** ($p < 0.001$), or **** ($p < 0.0001$).

Author contributions

AvS, AJO, IvdB, IvdB, KN, NRR, ST, UK performed experiments and analysed data. AS and CM conceived the study, designed and performed experiments, analysed the data, supervised and coordinated the study, and wrote the paper.

Declaration of Competing Interest

The authors declare no competing interests.

Acknowledgements

We are grateful to John Collard, Ellen van der Schoot, Ken Yamada, and Jari Ylanne for their generous gifts of reagents. Moreover, we gratefully acknowledge technical support from Pablo Secades (Netherlands Cancer Institute, Amsterdam), Anita Pfauth and Frank van Diepen (flow cytometry facility, Netherlands Cancer Institute Amsterdam), Ben Morris and Roderick Beijersbergen (Robotics and Screening Center, Netherlands Cancer Institute, Amsterdam), Jos van Rijssel (Sanquin Research, Amsterdam), Mark Hoogenboezem and Erik

Mul (Central Facility, Sanquin Research, Amsterdam), and Lenny Brocks and Marjolijn Mertz (Digital microscopy facility, Netherlands Cancer Institute, Amsterdam). Work in CM's laboratory is supported by The Netherlands Organization for Scientific Research (ZonMW Veni 016.146.160) and the Dutch Thrombosis Foundation (TSN 2017-01).

References

[1] K. Campbell, J. Casanova. A common framework for EMT and collective cell migration. *Development,* 143 (2016), pp. 4291-4300.
[2] P. Friedl, R. Mayor. Tuning collective cell migration by cell-cell junction regulation. *Cold Spring Harb. Perspect. Biol*., 9 (2017), p. 4.
[3] M.M. Zegers, P. Friedl. Rho GTPases in collective cell migration. *Small GTPases*, 5 (2014), p. e28997.
[4] R. Pankov, Y. Endo, S. Even-Ram, M. Araki, K. Clark, E. Cukierman, K. Matsumoto, K. Yamada. A Rac switch regulates random versus directionally persistent cell migration. *J. Cell Biol.,* 170 (2005), pp. 793-802.
[5] V. Sanz-Moreno, G. Gadea, J. Ahn, H. Paterson, P. Marra, S. Pinner, E. Sahai, C. Marshall. Rac activation and inactivation control plasticity of tumor cell movement. *Cell,* 135 (2008), pp. 510-523.
[6] A. Ridley. Rho GTPase signalling in cell migration. *Curr. Opin. Cell Biol*., 36 (2015), pp. 103-112.
[7] A. Ratheesh, R. Priya, A.S. Yap. Coordinating Rho and Rac: the regulation of Rho GTPase signaling and cadherin junctions. *Prog. Mol. Biol. Transl. Sci*., 116 (2013), pp. 49-68.
[8] J. McCormack, N.J. Welsh, V.M. Braga. Cycling around cell-cell adhesion with Rho GTPase regulators. *J. Cell Sci*., 126 (2013), pp. 379-391.
[9] F. Libanje, J. Raingeaud, R. Luan, Z. Thomas, O. Zajac, J. Veiga, L. Marisa, J. Adam, V. Boige, D. Malka, D. Goéré, A. Hall, J. Soazec, F. Prall, M. Gelli, P. Dartigues, F. Jaulin. ROCK2 inhibition triggers the collective invasion of colorectal adenocarcinomas. *EMBO J.,* 38 (2019), p. e99299.
[10] N. Gjorevski, A.S. Piotrowski, V.D. Varner, C.M. Nelson. Dynamic tensile forces drive collective cell migration through three-dimensional extracellular matrices. *Sci. Rep*., 5 (2015), p. 11458.
[11] C. Gaggioli, S. Hooper, C. Hidalgo-Carcedo, R. Grosse, J. Marshall, K. Harrington, E. Sahai. Fibroblast-led collective invasion of carcinoma cells with differing roles for RhoGTPases in leading and following cells. *Nat. Cell Biol*., 9 (2007), pp. 1392-1400.
[12] A.J. Ewald, A. Brenot, M. Duong, B.S. Chan, Z. Werb. Collective epithelial migration and cell rearrangements drive mammary branching morphogenesis. *Dev. Cell,* 14 (2008), pp. 570-581.
[13]. C. Collins, W.J. Nelson. Running with neighbors: coordinating cell migration and cell-cell adhesion. *Curr. Opin. Cell Biol*., 36 (2015), pp. 62-70.
[14] M. Reffay, M. Parrini, O. Cochet-Escartin, B. Ladoux, A. Buguin, S. Coscoy, F. Amblard, J. Camonis, P. Silberzan. Interplay of RhoA and mechanical forces in collective cell migration driven by leader cells. *Nat. Cell Biol.,* 16 (2014), pp. 217-223.
[15] E. Vandenbroucke, D. Mehta, R. Minshall, A.B. Malik. Regulation of endothelial junctional permeability. *Ann. N. Y. Acad. Sci.,* 1123 (2008), pp. 134-145.
[16] J. Oldenburg, J. de Rooij. Mechanical control of the endothelial barrier. *Cell Tissue Res*., 355 (2014), pp. 545-555.
[17] S.E. Winograd-Katz, R. Fassler, B. Geiger, K.R. Legate. The integrin adhesome: from genes and proteins to human disease. *Nat. Rev. Mol. Cell Biol*., 15 (2014), pp. 273-288.

[18] D.A. Calderwood, I.D. Campbell, D.R. Critchley. Talins and kindlins: partners in integrin-mediated adhesion. *Nat. Rev. Mol. Cell Biol*., 14 (2013), pp. 503-517.
[19] H. Yamamoto, M. Ehling, K. Kato, K. Kanai, M. van Lessen, M. Frye, D. Zeuschner, M. Nakayama, D. Vestweber, R.H. Adams. Integrin beta1 controls VE-cadherin localization and blood vessel stability. *Nat. Commun*., 6 (2015), p. 6429.
[20] J. de Rooij, A. Kerstens, G. Danuser, M.A. Schwartz, C.M. Waterman-Storer. Integrin-dependent actomyosin contraction regulates epithelial cell scattering *J. Cell Biol*., 171 (2005), pp. 153-164.
[21] .L. Mui, C.S. Chen, R.K. Assoian. The mechanical regulation of integrin-cadherin crosstalk organizes cells, signaling and forces. *J. Cell Sci*., 129 (2016), pp. 1093-1100.
[22] M.A. Glukhova, J.P. Thiery. Fibronectin and integrins in development. *Semin. Cancer Biol.*, 4 (1993), pp. 241-249.
[23] P. Rousselle, M. Montmasson, C. Garnier. Extracellular matrix contribution to skin wound re-epithelialization. *Matrix Biol.,* 75–76 (2019), pp. 12-26.
[24] R.O. Hynes, J. Lively, J. McCarty, D. Taverna, S. Francis, K. Hodivala-Dilke, Q. Xiao. The diverse roles of integrins and their ligands in angiogenesis. *Cold Spring Harb. Symp. Quant. Biol*., 67 (2002), pp. 143-153.
[25] A.E. Sutherland, P.G. Calarco, C.H. Damsky. Developmental regulation of integrin expression at the time of implantation in the mouse embryo. *Development*, 119 (1993), pp. 1175-1186.
[26] H.B. Schiller, M. Hermann, J. Polleux, T. Vignaud, S. Zanivan, C. Friedel, Z. Sun, A. Raducanu, K. Gottschalk, M. Théry, M. Mann, R. Fässler. beta1- and alphav-class integrins cooperate to regulate myosin II during rigidity sensing of fibronectin-based microenvironments. *Nat. Cell Biol.,* 15 (2013), pp. 625-636.
[27] M. Bharadwaj, N. Strohmeyer, G. Colo, J. Helenius, N. Beerenwinkel, H. Schiller, R. Fässler, D. Müller. alphaV-class integrins exert dual roles on alpha5beta1 integrins to strengthen adhesion to fibronectin. *Nat. Commun*., 8 (2017), p. 14348.
[28] N. Strohmeyer, M. Bharadwaj, M. Costell, R. Fassler, D. Muller. Fibronectin-bound alpha5beta1 integrins sense load and signal to reinforce adhesion in less than a second. *Nat. Mater.,* 16 (2017), pp. 1262-1270.
[29] A.J. Woods, D.P. White, P.T. Caswell, J.C. Norman. PKD1/PKCmu promotes alphavbeta3 integrin recycling and delivery to nascent focal adhesions. *EMBO J.,* 23 (2004), pp. 2531-2543.
[30] D.P. White, P.T. Caswell, J.C. Norman. alphavbeta3 and and alpha5beta1 integrin recycling pathways dictate downstream Rho kinase signaling to regulate persistent cell migration. *J. Cell Biol.,* 177 (2007), pp. 515-525.
[31] O. Rossier, V. Octeau, S.J. B, C. Leduc, B. Tessier, D. Nair, V. Gatterdam, O. Destaing, C. Albigès-Rizo, R. Tampé, L. Cognet, D. Choquet, B. Lounis, G. Giannone. Integrins beta1 and beta3 exhibit distinct dynamic nanoscale organizations inside focal adhesions. *Nat. Cell Biol*., 10 (2012), pp. 1057-1067.
[32] H.E. Balcioglu, H. van Hoorn, D.M. Donato, T. Schmidt, E.H. Danen. The integrin expression profile modulates orientation and dynamics of force transmission at cell-matrix adhesions. *J. Cell Sci*., 128 (2015), pp. 1316-1326.
[33] G.L. Lin, D.M. Cohen, R.A. Desai, B.M. T, L. Gao, M.J. Humphries, C.S. Chen. Activation of beta1 but not beta3 integrin increases cell traction forces. *FEBS Lett*., 587 (2013), pp. 763-769.
[34] D.C. Worth, K. Hodivala-Dilke, S.D. Robinson, S.J. King, P.E. Morton, F.B. Gertler, M.J. Humphries, M. Parsons. alphavbeta3 integrin spatially regulates VASP and RIAM to control adhesion dynamics and migration. *J. Cell Biol*., 189 (2010), pp. 369-383.

[35] C. Jonker, R. Galmes, T. Veenendaal, C. Brink, R. van der Welle, N. Liv, J. de Rooij, A.A. Peden, P. van der Sluijs, C. Margadant, J. Klumperman. Vps3 and Vps8 control integrin trafficking from early to recycling endosomes and regulate integrin-dependent functions. *Nat. Commun*., 9 (2018), pp. 1-12.
[36] C. Gimond, A. van Der Flier, S. van Delft, C. Brakebusch, I. Kuikman, J.G. Collard, R. Fässler, A. Sonnenberg. Induction of cell scattering by expression of beta1-integrins in beta1-deficient epithelial cells requires activation of members of the rho family of GTPases and downregulation of cadherin and catenin function. *J. Cell Biol*., 147 (1999), pp. 1325-1340.
[37] E.H. Danen, P. Sonneveld, C. Brakebusch, R. Fassler, A. Sonnenberg. The fibronectin-binding integrins alpha5beta1 and alphavbeta3 differentially modulate RhoA-GTP loading, organization of cell matrix adhesions, and fibronectin fibrillogenesis. *J. Cell Biol*., 159 (2002), pp. 1071-1086
[38] E.H. Danen, J. van Rheenen, W. Franken, S. Huveneers, P. Sonneveld, K. Jalink, A. Sonnenberg. Integrins control motile strategy through a Rho-cofilin pathway. *J. Cell Biol*., 169 (2005), pp. 515-526.
[39] C. Margadant, I. van den Bout, A.L. van Boxtel, V.L. Thijssen, A. Sonnenberg. Epigenetic regulation of galectin-3 expression by β1 integrins promotes cell adhesion and migration. *J. Biol Chem*., 287 (2012), pp. 44684-44693.
[40] C. Margadant, M. Kreft, D.J. de Groot, J.C. Norman, A. Sonnenberg. Distinct roles of talin and kindlin in regulating integrin alpha5beta1 function and trafficking. *Curr. Biol*., 22 (2012), pp. 1554-1563.
[41] M. Moser, K.R. Legate, R. Zent, R. Fassler. The tail of integrins, talin, and kindlins. *Science*, 324 (2009), pp. 895-899.
[42] K. Bledzka, J. Liu, Z. Xu, H.D. Perera, S.P. Yadav, K. Bialkowska, J. Qin, Y.Q. Ma, E.F. Plow. Spatial coordination of kindlin-2 with talin head domain in interaction with integrin beta cytoplasmic tails. *J. Biol Chem*., 287 (2012), pp. 24585-24594.
[43] Z. Liao, H. Kato, M. Pandey, J.M. Cantor, A.J. Ablooglu, M.H. Ginsberg, S.J. Shattil. Interaction of kindlin-2 with integrin beta3 promotes outside-in signaling responses by the alphaVbeta3 vitronectin receptor. *Blood,* 125 (2015), pp. 1995-2004.
[44] B. Wojciak-Stothard, S. Potempa, T. Eichholtz, A.J. Ridley. Rho and Rac but not Cdc42 regulate endothelial cell permeability. *J. Cell Sci*., 114 (2001), pp. 1343-1355.
[45] C.M. Beckers, V.W. van Hinsbergh, G.P. van Nieuw Amerongen. Driving Rho GTPase activity in endothelial cells regulates barrier integrity. Thromb. Haemost., 103 (2010), pp. 40-55.
[46] S. Huveneers, J. Oldenburg, E. Spanjaard, G. van der Krogt, I. Grigoriev, A. Akhmanova, H. Rehmann, J. de Rooij. Vinculin associates with endothelial VE-cadherin junctions to control force-dependent remodelling. *J. Cell Biol*., 196 (2012), pp. 641-652.
[47] J.D. van Buul, D. Geerts, S. Huveneers. Rho GAPs and GEFs: controling switches in endothelial cell adhesion. *Cell Adhes. Migr*., 8 (2014), pp. 108-124.
[48] M.N. Nakatsu, C.C. Hughes. An optimised three-dimensional in vitro model for the analysis of angiogenesis. *Methods Enzym*., 443 (2008), pp. 65-82.
[49] J. Rossant, J.C. Cross. Placental development: lessons from mouse mutants. *Nat. Rev. Genet*., 2 (2001), pp. 538-548.
[50] C.H. Graham, T.S. Hawley, R.G. Hawley, J.R. MacDougall, R.S. Kerbel, N. Khoo, P.K. Lala. Establishment and characterization of first trimester human trophoblast cells with extended lifespan. *Exp. Cell Res.,* 206 (1993), pp. 204-211.
[51] M. Theodosiou, M. Widmaier, R.T. Böttcher, E. Rognoni, M. Veelders, M. Bharadwaj, A. Lambacher, K. Austen, D.J. Müller, R. Zent, R. Fässler. Kindlin-2 cooperates with talin to activate integrins and induces cell spreading by directly binding paxillin. *Elife*, 5 (2016), p. e10130.

[52] R.T. Bottcher, M. Veelders, P. Rombaut, J. Faix, M. Theodosiou, T.E. Stradal, K. Rottner, R. Zent, F. Herzog, R. Fässler. Kindlin-2 recruits paxillin and Arp2/3 to promote membrane protrusions during initial cell spreading. *J. Cell Biol*., 216 (2017), pp. 3785-3798.
[53] M. Yasuda-Yamahara, M. Rogg, J. Frimmel, P. Trachte, M. Helmstaedter, P. Schroder, M. Schiffer, C. Schell, T.B. Huber. FERMT2 links cortical actin structures, plasma membrane tension and focal adhesion function to stabilize podocyte morphology. *Matrix Biol*., 68–69 (2018), pp. 263-279.
[54] R. Postel, C. Margadant, B. Fischer, M. Kreft, H. Janssen, P. Secades, G. Zambruno, A. Sonnenberg. Kindlin-1 mutant zebrafish as an in vivo model system to study adhesion mechanisms in the epidermis. *J. Investig. Dermatol*., 133 (2013), pp. 2180-2190.
[55] E. Pluskota, J.J. Dowling, N. Gordon, J.A. Golden, D. Szpak, X.Z. West, C. Nestor, Y. Ma, K. Bialkowska, T. Byzova, E.F. Plow. The integrin coactivator Kindlin-2 plays a critical role in angiogenesis in mice and zebrafish. *Blood*, 117 (2011), pp. 4978-4987.
[56] S.A. Wickstrom, A. Lange, E. Montanez, R. Fassler. The ILK/PINCH/parvin complex: the kinase is dead, long live the pseudokinase! *EMBO J*., 29 (2010), pp. 281-291.
[57] E. Montanez, S. Wickstrom, J. Altstatter, H. Chu, R. Fassler. Alpha-parvin controls vascular mural cell recruitment to vessel wall by regulating RhoA/ROCK signalling. *EMBO J*., 28 (2009), pp. 3132-3144.
[58] G. Jacquemet, D.M. Green, R.E. Bridgewater, A. von Kriegsheim, M.J. Humphries, J.C. Norman, P.T. Caswell. RCP-driven alpha5beta1 recycling suppresses Rac and promotes RhoA activity via the RacGAP1-IQGAP1 complex. *J. Cell Biol*., 202 (2013), pp. 917-935.
[59] B. Nieves, C.W. Jones, R. Ward, Y. Ohta, C.G. Reverte, S.E. LaFlamme. The NPIY motif in the integrin β1 tail dictates the requirement for talin-1 in outside-in signalling. *J. Cell Sci*., 123 (2010), pp. 1216-1226.
[60] A.J. Ridley. Rho GTPase signalling in cell migration. *Curr. Opin. Cell Biol*., 36 (2015), pp. 103-112.
[61] A.W. Orr, M.H. Ginsberg, S.J. Shattil, H. Deckmyn, M.A. Schwartz. Matrix-specific suppression of integrin activation in shear stress signalling. *Mol. Biol. Cell*, 17 (2006), pp. 4686-4697.
[62] D.P. Ly, K.M. Zazzali, S.A. Corbett..De novo expression of the integrin alpha5beta1 regulates alphavbeta3-mediated adhesion and migration on fibrinogen. *J. Biol. Chem.,* 278 (2003), pp. 21878-21885.
[63] D.A. Calderwood, V. Tai, G. DiPaolo, P. DeCamilli, M.H. Ginsberg. Competition for talin results in trans-dominant inhibition of integrin activation. *J. Biol Chem*., 279 (2004), pp. 28889-28895.
[64] Y. Mao, J. Schwarzbauer. Accessibility to the fibronectin synergy site in a 3D matrix regulates engagement of alpha5beta1 versus alphavbeta3 integrin receptors. *Cell Commun. Adhes*., 13 (2006), pp. 267-277.
[65] M. Benito-Jardón, S. Klapproth, I. Gimeno-LLuch, T. Petzold, M. Bharadwaj, D. Müller, G. Zuchtriegel, C. Reichel, M. Costell. The fibronectin synergy site re-enforces cell adhesion and mediates a crosstalk between integrin classes. *Elife*, 6 (2017), p. e22264.
[66] Y. Mao, J. Schwarzbauer. Fibronectin fibrillogenesis, a cell-mediated matrix assembly process. *Matrix Biol.,* 24 (2005), pp. 389-399.
[67] S. Huveneers, H. Truong, R. Fässler, A. Sonnenberg, E.H.J. Danen. Binding of soluble fibronectin to integrin alpha5beta1– link to focal adhesion redistribution and contractile shape. *J. Cell Sci*. (2008), pp. 2452-2462.
[68] J.M. Linton, G.R. Martin, L.F. Reichardt. The ECM protein nephronectin promotes kidney development via integrin alpha8beta1-mediated stimulation of Gdnf expression. *Development,* 2509 (2007), pp. 2501-2509.

[69] X.Z. Huang, J.F. Wu, R. Ferrando, J.H. Lee, Y.L. Wang, R.V. F.arese, D. Sheppard. Fatal bilateral chylothorax in mice lacking the integrin alpha9beta1. *Mol. Cell Biol.,* 20 (2000), pp. 5208-5215.
[70] J.T. Yang, H. Rayburn, R.O. Hynes. Cell adhesion events mediated by α 4 integrins are essential in placental and cardiac development. *Development,* 560 (1995), pp. 549-560.
[71] A. Capuano, E. Pivetta, F. Baldissera, G. Bosisio, B. Wassermann, F. Bucciotti, A. Colombatti, P. Sabatelli, R. Doliana, P. Spessotto. Integrin binding site within the gC1q domain orchestrates EMILIN-1-induced lymphangiogenesis. *Matrix Biol*., 81 (2019), pp. 34-49.
[72] A. Capuano, F. Fogolari, F. Bucciotti, P. Spessotto, P. Nicolosi, M. Mucignat, M. Cervi, G. Esposito, A. Colombatti, R. Doliana. The alpha4beta1/EMILIN1 interaction discloses a novel and unique integrin-ligand type of engagement. *Matrix Biol*., 66 (2018), pp. 50-66.
[73] J.T. Yang, H. Rayburn, R.O. Hynes. Embryonic mesodermal defects in integrin-deficient mice. *Development*, 1105 (1993), pp. 1093-1105.
[74] N.I. Reed, H. Jo, C. Chen, K. Tsujino, T.D. Arnold, W.F. Degrado, D. Sheppard. The alphavbeta1 integrin plays a critical in vivo role in tissue fibrosis. *Sci. Transl. Med*. (2015), p. 7.
[75] T. Pietri, J.P. Thiery, S. Dufour. Differential expression of beta3 integrin gene in chick and mouse cranial neural crest cells. *Dev. Dyn.,* 227 (2003), pp. 309-313.
[76] D. Liang, X. Wang, A. Mittal, S. Dhiman, S.Y. Hou, K. Degenhardt, S. Astrof. Mesodermal expression of integrin alpha5beta1 regulates neural crest development and cardiovascular morphogenesis. *Dev. Biol*., 395 (2014), pp. 232-244.
[77] A. Mittal, M. Pulina, S.Y. Hou, S. Astrof. Fibronectin and integrin alpha5 play essential roles in the development of the cardiac neural crest. *Mech. Dev*., 127 (2010), pp. 472-484.
[78] D. Alfandari, H. Cousin, A. Gaultier, B.G. Hoffstrom, D.W. DeSimone. Integrin alpha5beta1 supports the migration of Xenopus cranial neural crest on fibronectin. *Dev. Biol*., 260 (2003), pp. 449-464.
[79] Y. Endo, H. Ishiwata-Endo, K. Yamada. Cloning and characterization of chicken α5 integrin: endogenous and experimental expression in early chicken embryos. *Matrix Biol*., 32 (2013), pp. 381-386.
[80] M.R. Clay, M.C. Halloran. Rho activation is apically restricted by Arhgap1 in neural crest cells and drives epithelial-to-mesenchymal transition. *Development,* 140 (2013), pp. 3198-3209.
[81] Y. Zhang, T.H. Kim, L. Niswander. Phactr4 regulates directional migration of enteric neural crest through PP1, integrin signaling, and cofilin activity. *Genes Dev*., 26 (2012), pp. 69-81.
[82] G. Serini, D. Valdembri, F. Bussolino. Integrins and angiogenesis: a sticky business. *Exp. Cell Res*., 312 (2006), pp. 651-658.
[83] F. Demircioglu, K. Hodivala-Dilke. alphavbeta3 integrin and tumour blood vessels-learning from the past to shape the future. *Curr. Opin. Cell Biol.,* 42 (2016), pp. 121-127.
[84] G.H. Mahabeleshwar, W. Feng, K. Reddy, E.F. Plow, T.V. B.yzova. Mechanisms of integrin-vascular endothelial growth factor receptor cross-activation in angiogenesis. *Circ. Res*., 101 (2007), pp. 570-580.
[85] A.R. Reynolds, L.E. Reynolds, T.E. Nagel, J.C. Lively, S.D. Robinson, D.J. Hicklin, S.C. Bodary, K.M. Hodivala-Dilke. Elevated Flk1 (vascular endothelial growth factor receptor 2) signaling mediates enhanced angiogenesis in beta3-integrin-deficient mice. *Cancer Res.,* 64 (2004), pp. 8643-8650.
[86] L.E. Reynolds, L. Wyder, J.C. Lively, D. Taverna, S.D. Robinson, X. Huang, D. Sheppard, R.O. Hynes, K.M. Hodivala-Dilke. Enhanced pathological angiogenesis in mice lacking beta3 integrin or beta3 and beta5 integrins. *Nat. Med*. (2002), pp. 27-34.

[87] A. van der Flier, K. Badu-Nkansah, C.A. Whittaker, D. Crowley, R.T. Bronson, A. Lacy-Hulbert, R.O. Hynes. Endothelial alpha5 and alphav integrins cooperate in remodeling of the vasculature during development. Development, 137 (2010), pp. 2439-2449.
[88] B.L. Bader, H. Rayburn, D. Crowley, R.O. Hynes. Extensive vasculogenesis, angiogenesis, and organogenesis precede lethality in mice lacking all alphav integrins. *Cell*, 95 (1998), pp. 507-519.
[89] G. Su, A. Atakilit, J.T. Li, N. Wu, M. Bhattacharya, J. Zhu, J.E. Shieh, E. Li, R. Chen, S. Sun, C.P. Su, D. Sheppard. Absence of integrin alphavbeta3 enhances vascular leak in mice by inhibiting endothelial cortical actin formation. *Am J Respir Crit Care Med*, 185 (2012), pp. 58-66.
[90] L. Hakanpaa, E.A. Kiss, G. Jacquemet, I. Miinalainen, M. Lerche, C. Guzmán, E. Mervaala, L. Eklund, J. Ivaska, P. Saharinen. Targeting beta1-integrin inhibits vascular leakage in endotoxemia. *Proc. Natl. Acad. Sci. USA*, 115 (2018), pp. E6467-E6476.
[91] L. Hakanpaa, T. Sipila, V.M. Leppanen, P. Gautam, H. Nurmi, G. Jacquemet, L. Eklund, J. Ivaska, K. Alitalo, P. Saharinen. Endothelial destabilization by angiopoietin-2 via integrin beta1 activation. *Nat. Commun.*, 6 (2015), p. 5962.
[92] I. van den Bout, H.H. Truong, S. Huveneers, I. Kuikman, E.H. Danen, A. Sonnenberg. The regulation of MacMARCKS expression by integrin beta3. *Exp. Cell Res.*, 313 (2007), pp. 1260-1269.
[93] C. Margadant, M. Kreft, G. Zambruno, A. Sonnenberg. Kindlin-1 regulates integrin dynamics and adhesion turnover. *PLoS One*, 8 (2013), pp. 1-10.
[94] E. Sander, J.P. ten Klooster, S. van Delft, R.A. van der Kammen, J.G. Collard. Rac downregulates Rho activity: reciprocal balance between both GTPases determines cellular morphology and migratory behaviour. *J. Cell Biol.*, 147 (1999), pp. 1009-1021.